 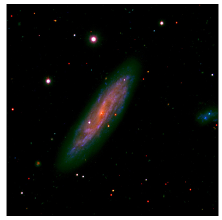 LBT & Image

"AUGER ELECTRONS VIA K_α X-RAY LINES OF PLATINUM COMPOUNDS FOR NANOTECHNOLOGICAL APPLICATIONS"

Sultana N. Nahar
Astronomy

Sara Lim, Biophysics, Anil K. Pradhan, Astronomy,
Russ M. Pitzer, Chemistry,
Collaborators: Enam Chowdhury, D. Wertepny, Physics
E. Bell, N. Gupta, A. Chakraborty, Radiation Oncology
Y. Yan and team, Thomas Jefferson U.

"66th International Symposium on Molecular Spectroscopy"
Ohio State University, Columbus, Ohio, USA
June 22-26, 2011
Supports: NASA APRA, DOE
Computations - Ohio Supercomputer Center (OSC)

RESONANT THERANOSTICS (RT): Progress

RT Objective:

- **Use of high-Z nanoparticles (e.g. gold) with X-ray radiation is more effective in radiation therapy than pure irradiation - Ejected electrons from the nanoparticles destroy the surrounding malignant cells**
- **Conventional biomedical methods use intense and broadband high energy X-rays in therapy and diagnostics (theranostics) imaging or treatment to ensure sufficient tissue penetration**
- **To avoid damages incurred by these, RT, aims to find narrow energy regions that correspond to *resonant* absorption or emission**

PRESENT:

- **X-ray spectroscopy of Pt compound (cisplatin) commonly used in medicine, e.g. Chemotherapy**

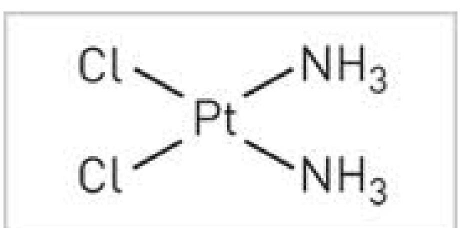

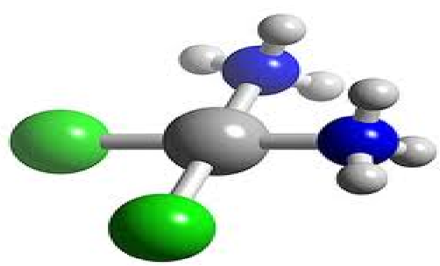

- **High energy X-rays intereact only with Pt in cisplatin as Pt can absorb or emit these photons**
- **Obtained resonant energy, E_{res}=64 - 70 keV, when Pt goes through 1s-2p transitions**
- **Obtained oscillator strengths (f), transition probabilities or decay rates (A) and photon absorption coefficients per unit mass ($\kappa = \sigma/\mathrm{m}$) for Resonant Transitions in H- to F-like Pt**

Illustrate:

• **At the resonant energies, the attenuation or absorption coefficients κ are orders of magnitude higher than both the background and that at K-shell ionization energy (E_K)**

$\rightarrow$ **Research should focus on Resonant energy band, $\mathbf{E}_{res}$ which is lie *below* the K-shell ionization energy, instead on the E_K itself**

• **Targeting these energy bands with a tunable monochromatic X-ray source, Auger processes can be initiated to produce large number of photons and electrons via photon fluorescence and electron ejections**

• **Detected monochromatic $\mathbf{K}_{\alpha}$ X-rays from Zr from an X-ray machine**

RT METHOD: NANOBIO-SPECTROSCOPY

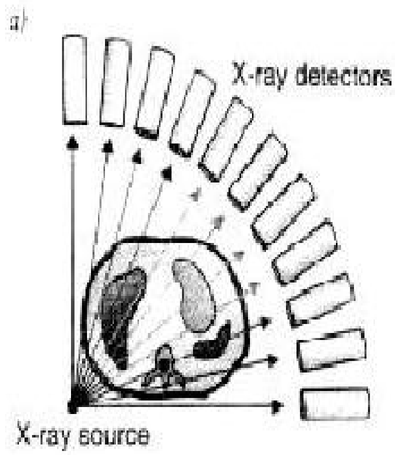

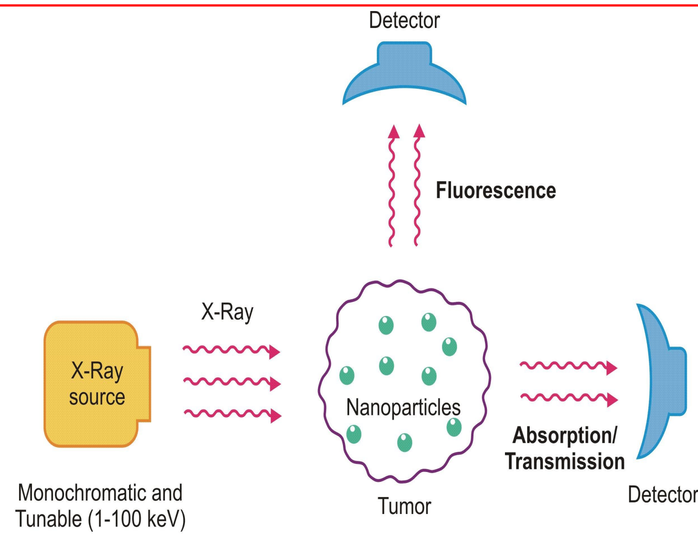

- Full body CAT scans use high energy broad band X-rays with very high radiation dosages (left Fig)
- Broadband imaging yields pictures - Spectroscopy gives more detailed microscopic and accurate information
- Spectroscopically targeted radiation should be far more efficient with reduced exposure
- RT Method: Tumors are doped with nanoparticles of heavy elements for breakup of DNA of tumor cells by X-rays (right Fig)
- Heavy elements absorb/emit X-rays at higher energies where biogenic elements (H,C,N,O,CHON) are transparent
- Direct X-ray impact by a tunable monochromatic X-ray source and absorption by nanoparticles at resonant energies
- Fluorescent emission and electron ejections due to inner-shell ionization following brief impact
- Need a tunable monochromatic X-ray source

Auger Cascade: ELECTRON & PHOTON EMISSIONS

Auger Process: An electron from a higher level drops to fill a lower level vacancy, but emits a photon that can knock out another electron. This can lead to cascade as the vacancies move upward, more electrons and photons are emitted.

- **Fig (i) Ionization by X-ray photons (E_X) (> K-shell ionization energy E_K) leading to Auger process**
- **Fig (ii) Multiple electron vacancies due to successive Auger decays leading to emission of photons and electrons**
- **Single ionization of 1s electron can lead to ejection of 20 or more electrons in an ion with occupied O and P shells**
- **Fig (iii) Inverse to Auger - Resonant photo-excitation from 1s → 2p (with L-shell vacancy) by an external monoenergetic X-ray source with intensity above our predicted critical flux**

$$\mathbf{\Phi^c(\nu_{K\alpha}) = \frac{\sum_{n_i \geq 2} g_i A[n_i(S_iL_iJ_i) \to 2(SLJ)]}{g_K B_{K\alpha}}}. \quad (1)$$

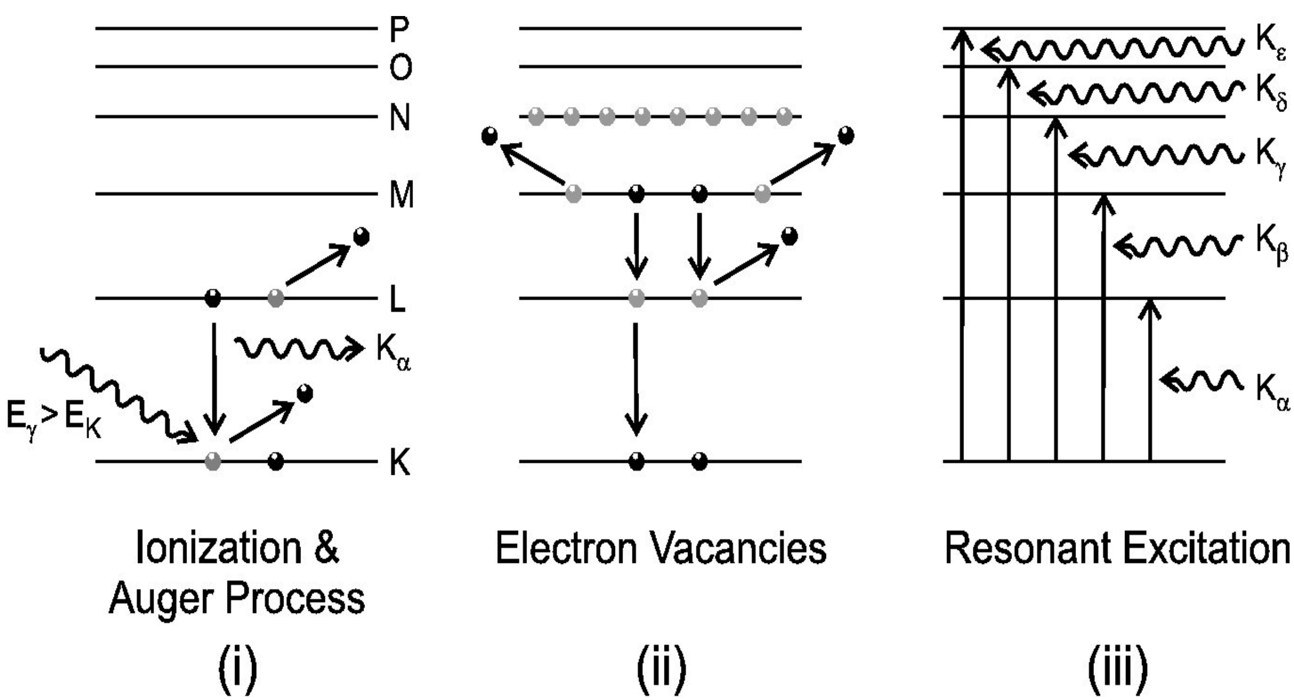

RESONANT K_α (1s-2p) TRANSITIONS IN Pt

- **Auger cascades are initiated with K-shell ionization leading to various ionic states**
- **The table presents data for resonant $K-$shell $(1s-2p)$ transitions for various ionic states of Pt**

Pt:$(1s^2 2s^2 2p^6 3s^2 3p^6 3d^{10} 4s^2 4p^6 4d^{10} 4f^{14} 5s^2 5p^6 5d^9 6s)$

- $E(K_\alpha)$**= averaged resonant energy (LS),** f_{tot}**= total oscillator strength,** σ_{res}**= photoionization cross section,** κ**= photo-absorption coefficient**
- **K_α resonance strengths contribute to photo-absorption (κ), far more than K-shell ionization (κ= 8.98 cm^2/g at E_K= 78.39 keV)(Nahar, Pradhan, Lim 2011)**

Transition Array	Ionic State	# of Transitions	$E(K_\alpha)$ (keV)	f_{tot}	$\langle\sigma_{res}(K_\alpha)\rangle$ (Mb)	κ cm^2/g
			Pt			
$1s-2p$	H	2	68.071	2.95E-01	2.38E+00	7.35E+03
$1s^2-1s2p$	He	2	67.746	5.83E-01	4.71E+00	1.45E+04
$1s^22s-1s2s2p$	Li	6	67.666	5.71E-01	4.60E+00	1.42E+04
$1s^22s^2-1s2s^22p$	Be	2	67.726	5.09E-01	4.10E+00	1.27E+04
$1s^22s^22p-1s2s^22p^2$	B	14	67.061	9.03E-01	7.28E+00	2.25E+04
$1s^22s^22p^2-1s2s^22p^3$	C	35	66.831	1.70E+00	1.37E+01	4.24E+04
$1s^22s^22p^3-1s2s^22p^4$	N	35	66.803	1.26E+00	1.02E+01	3.14E+04
$1s^22s^22p^4-1s2s^22p^5$	O	14	67.122	8.09E-01	6.52E+00	2.01E+04
$1s^22s^22p^5-1s2s^22p^6$	F	2	66.744	1.65E-01	1.33E+00	4.10E+03

Photo-Absorption Coefficient $\kappa(\mathrm{cm}^2/\mathrm{g})$: $\mathrm{Pt} + h\nu \rightarrow \mathrm{Pt}^+ + \mathrm{e}$

- **Blue curve: Background κ**
- **Enhancements in κ $\rightarrow$ at K, L, M (sub)-shells ionization energies: E_K, E_L, E_M**
- **Rise at E_K, focus of experiments but without success, for enhanced emission of electrons**
- **K-α resonances (red), due to K $\rightarrow$ L excitations, are in E_{res} = 64 - 70 keV, below E_K**
- **Photo-absorption by these resonances exceed the background & jump at E_K by orders of magnitude $\rightarrow$ Increase in ejected electrons in E_{res}**

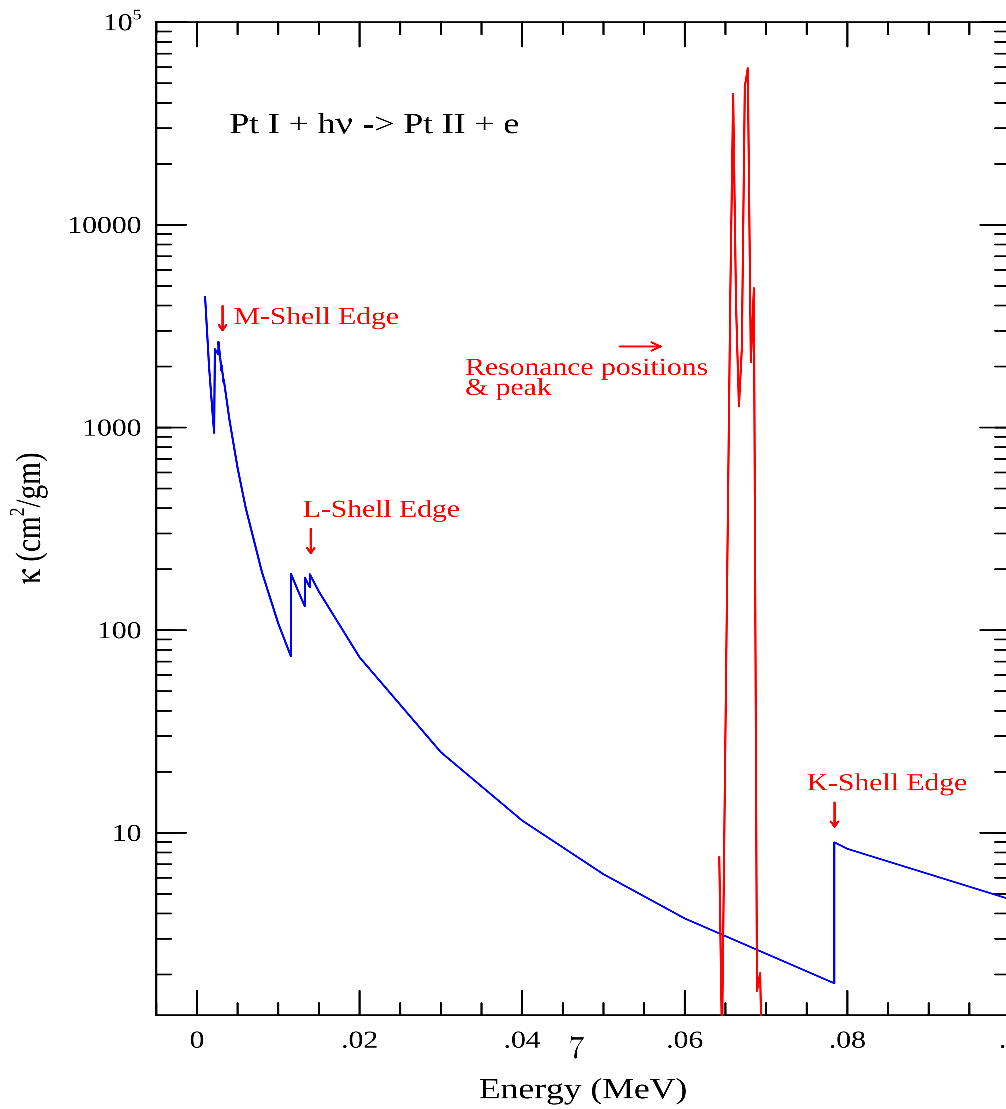

RADIATION FROM X-RAY MACHINES

- Bremsstrahlung radiation is emitted as electrons accelerate between cathode & anode of a given voltage and hit a high-Z target, e.g., tungsten (W)
- The energy range of the Bremsstrahlung varies from zero to the peak voltage of the machine
- Fig: Shape of Bremsstrahlung of elements, Al (green), Mo (turquoise) W(red), Au (blue)

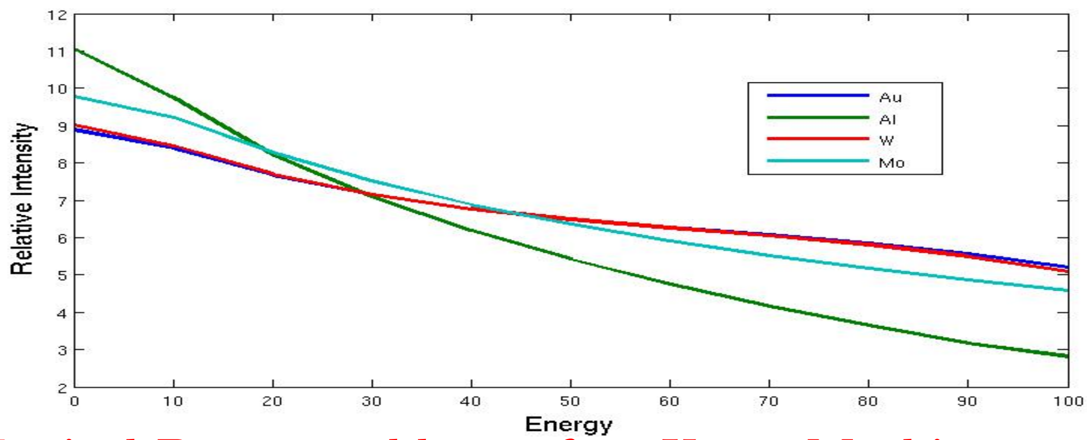

Typical Bremsstrahlung of an X-ray Machine

- A filter (e.g. Al) - reduces low energy radiation
- A typical Bremsstrahlung has a maximum at around 1/3 of the peak voltage
- Fig: Bremsstrahlung with W target & Al filter

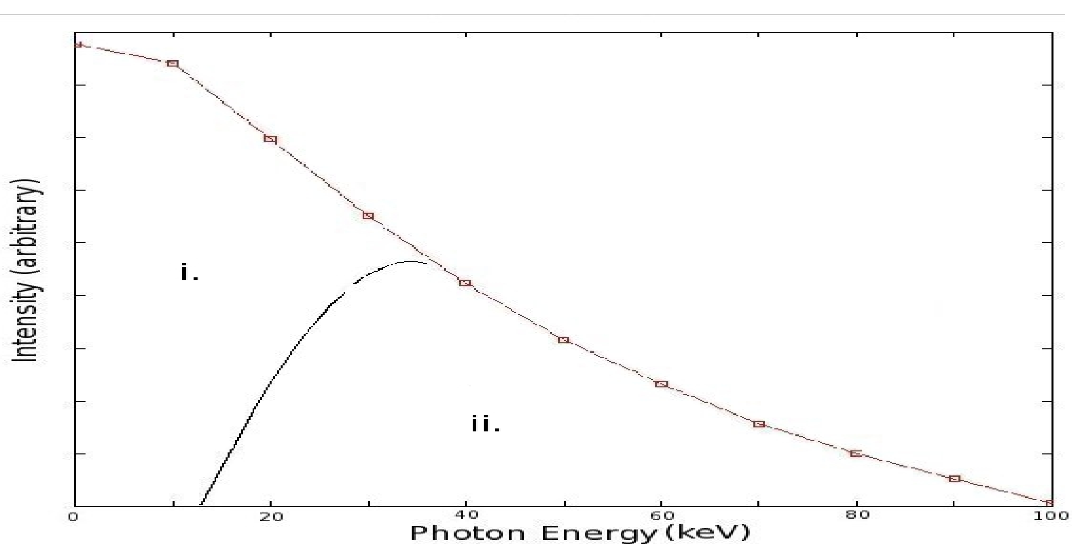

Monochromatic Radiation From an X-ray Machine

- Monochromatic radiation, such as, K_α can be produced when Bremsstrahlung of flux distribution f_B is directed to a high-Z target (X), rotated at a selective angle
- Inner K-shell ionization followed by radiative decays by upper shell electron can produce X-ray fluorescence at monochromatic energies.
- Figure: Production of K_α radiation from Zr (Pradhan et al 2010, unpublished)

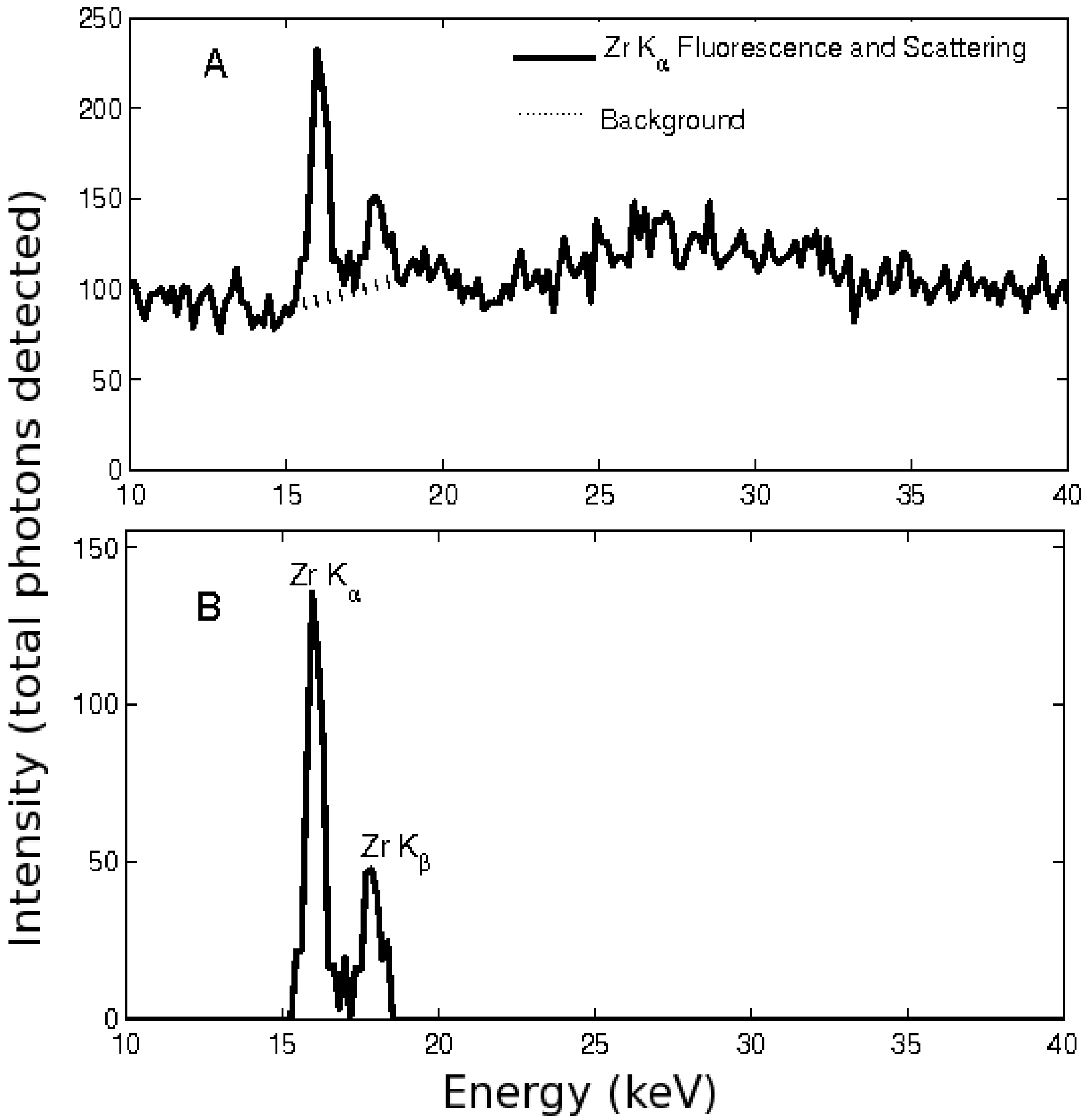

Flourescence Yield, Intensity of the Monochromatic Beam

• **The K-fluorescence yield (ω_K) can be estimated from the branching ratio:**

$$\omega_{\mathbf{K}} = \mathbf{A_r(L - K)/[A_r(L - K) + A_a(L)]}$$

A_r**(L - K) = Radiative decay rate for (L $\rightarrow$ K),** A_a **= Autoionization decay rate. For high-Z elements, e.f. Pt,** $\omega_K > 0.95$
$\rightarrow$ **All photons from the Bremsstrahlung source above the K-shell ionization energy, E > E_K, may be converted into monochromatic K_α radiation with high efficiency**

• **The estimated intensity of the monochromatic energy:**

$$\mathbf{I(K_\alpha) \sim N(X) \int_{E \geq E_K}^{E(kVp)} f_B \sigma_K(E) dE}$$

$N(X)$ **= number density,** σ_K **= K-shell photoionization cross section. For Zr: Efficiency of conversion ∼ 2%**

• **The monochromatic deposition of X-ray energy may then be localized using high-Z nanoparticles**

• **The RT scheme predicts considerable production of electron ejections and photon emissions via the Auger process and secondary CosterKronig and super-CosterKronig branching transitions**

CONCLUSION

1. We present X-ray spectroscopy of Pt in cisplatin where we predict resonant energies below the K-shell ionization threshold for enhanced X-ray absorption
2. We obtained Auger resonant probabilities and cross sections to obtain total mass attenuation coefficients with resonant cross sections
3. We find that the attenuation coefficients for X-ray absorptions at resonant energies are much larger, over orders of magnitude, higher over the background cross section as well as to that at K-edge threshold
4. We have been able to produce monochromatic radiation from the Bremsstrahlung of a conventional X-ray tube machine